

Magnetic Bond-Order Potential for Iron

M. Mrovec,^{1,2,*} D. Nguyen-Manh,³ C. Elsässer,^{1,2} and P. Gumbsch^{1,2}

¹IAM, Karlsruhe Institute of Technology, Kaiserstrasse 12, 76131 Karlsruhe, Germany

²Fraunhofer Institute for Mechanics of Materials IWM, Wöhlerstrasse 11, 79108 Freiburg, Germany

³EURATOM/CCFE Fusion Association, Culham Science Centre, Abingdon, OX14 3DB, United Kingdom

(Received 26 January 2011; published 14 June 2011)

We present a magnetic bond-order potential (BOP) that is able to provide a correct description of both directional covalent bonds and magnetic interactions in iron. This potential, based on the tight binding approximation and the Stoner model of itinerant magnetism, forms a direct bridge between the electronic-structure and the atomistic modeling hierarchies. Even though BOP calculations are computationally more demanding than those using common empirical potentials, the formalism can be used for studies of complex defect configurations in large atomic ensembles exceeding 10^5 atoms. Our studies of dislocations in α -Fe demonstrate that correct descriptions of directional covalent bonds and magnetism are crucial for a reliable modeling of these defects.

DOI: [10.1103/PhysRevLett.106.246402](https://doi.org/10.1103/PhysRevLett.106.246402)

PACS numbers: 71.15.Nc, 61.72.Lk, 62.20.-x, 71.20.Be

Iron and its compounds and alloys belong to the technologically most important materials. Efforts to model Fe-based materials at the atomic level have been growing rapidly in the last years not only to gain a better fundamental understanding but also to facilitate the design of advanced materials such as modern high-strength twinning- or transformation-induced-plasticity (TWIP/TRIP) steels. First-principles calculations, e.g., within the generalized gradient approximation of the density functional theory (DFT), are able to provide trustworthy predictions for small atomic ensembles. However, the development of accurate models of interatomic interactions that could capture subtleties of chemical bonding and still be applicable in large-scale atomistic studies presents a significant challenge.

The absence of reliable and computationally efficient models of interatomic interactions for iron stems from a difficulty to describe appropriately and simultaneously two key ingredients of its atomic bonding: (1) the unsaturated directional covalent bonds and (2) the magnetic effects. Most of the existing interatomic potentials for Fe are of central-force type, based on the embedded atom method or the Finnis-Sinclair schemes (e.g., Refs. [1–4]), that cannot provide a proper description of directional bonds. There have been attempts to include angle-dependent terms in classical potentials (see, e.g., Refs. [5,6]), but these models use mostly empirical functional forms and their parameterization requires complicated fitting strategies. A common characteristic of almost all classical interatomic potentials is a complete lack of magnetic interactions. These potentials are therefore neither able to describe the broad variety of magnetic phases of iron nor provide any information about local magnetic phenomena in the vicinity of crystal defects.

The crucial importance of magnetic effects for structural stability of iron phases was described by Hasegawa and

Pettifor almost 30 years ago [7]. A first successful attempt to incorporate a description of magnetism into an empirical model was done recently by Dudarev and Derlet [4]. These authors augmented the Finnis-Sinclair model with a Stoner model in order to account for changes of magnetic moments around interstitial defects in collision cascade simulations. Unfortunately, the central-force character led to a limited applicability of this potential in dislocation studies.

Aside from the classical potentials are recent Gaussian approximation potentials [8] that attempt to reproduce the Born-Oppenheimer potential energy surface for a large set of atomic configurations. These models can deliver accurate predictions (albeit at much higher computational cost than the classical potentials) but provide only limited physical insight into structure-bonding relationships and completely lack magnetism.

In this Letter, we present a novel magnetic bond-order potential (BOP) for iron, as the first interatomic potential that is able to provide a correct description of both the directional covalent bonds and the magnetic interactions in iron. The magnetic BOP is based on the tight binding (TB) approximation to the electronic structure and contains a description of magnetic interactions within the Stoner theory of itinerant magnetism [9]. We demonstrate that the model is not only able to predict correctly the stability of various magnetic phases in bulk iron but also the behavior of crystal defects such as dislocations with an accuracy comparable to electronic-structure methods. Even though BOP calculations are computationally more demanding than those using common empirical potentials, we show on the example of dislocation kinks that our model is able to simulate complex configurations of up to 10^5 atoms on a single processor and to capture energy differences of few tens of eV.

The theory of BOPs has been developed by Pettifor and co-workers [10–12] and the methodology has been

successfully applied in atomistic studies of extended defects in nonmagnetic transition metals and their alloys (see, e.g., Refs. [12–15]). Here we summarize only the crucial points of the magnetic BOP formalism and refer the reader to original papers and Ref. [16] for more details.

The BOP model is in its essence a tight binding scheme that is recast to provide a real-space $O(N)$ description of interactions between the atoms [10–12]. The validity of various TB approximations for modeling magnetic properties of Fe have been tested by several authors [17–21]. Since the cohesion in Fe is primarily governed by d - d bonding, it is sufficient to include only d orbitals within the spin-polarized TB treatment [18]. It was shown recently that such model is also fully transferable to the case of magnetic Fe-Cr alloys [22]. The distance dependencies of the $dd\sigma$, $dd\pi$, and $dd\delta$ bond integrals in our BOP model were derived by an atomic-orbital projection scheme that enables us to obtain them directly from DFT calculations in a rigorous and controlled way without any need of fitting [16,21]. The crucial connection between the real-space BOP formalism and the k -space quantum mechanics of electrons is carried through a continued fraction expansion of the diagonal Green's function matrix elements, which provides a link between self-returning bonding paths in the lattice and approximated local densities of states (LDOS's) on the atoms. Similarly as in other transition metals, we carried out the bond-order expansion to four recursion levels which gives a 9th moment representation of the LDOS's. This guarantees that all important features of the LDOS's are correctly reproduced and assures a reliable description of local bonding in bulk phases as well as in less ordered environments. A comparison of k -space TB and BOP densities of states for bcc and fcc phases is shown in Fig. 1. The accurate evaluation of spin-polarized LDOS's is crucial for a correct determination of the magnetic contributions within the Stoner model. The local Stoner criterion, $In_i(E_F) > 1$, for onset of a stable

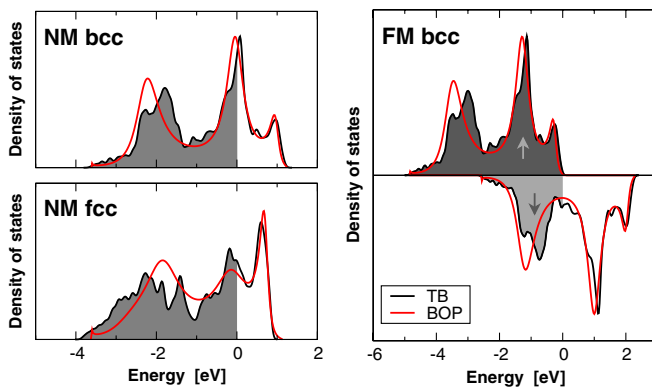


FIG. 1 (color online). Comparison of electronic densities of states for nonmagnetic (NM) bcc and fcc (left) and ferromagnetic (FM) bcc (right) Fe phases calculated using the k -space d-TB and 9th moment BOP theory. Shaded regions mark occupied states.

ferromagnetic state depends on the product of the Stoner exchange integral I and the LDOS at the Fermi level $n_i(E_F)$. Provided that $n_i(E_F)$ is correctly reproduced, the Stoner exchange integral is the only parameter that needs to be supplied into the BOP to capture all magnetic effects. Our value of $I = 0.80$ eV was again based on DFT calculations and adjusted to obtain a correct magnetic behavior within our d -only model. The right panel of Fig. 1 shows the spin density of states for the FM bcc phase obtained using the magnetic BOP, again agreeing well with the k -space TB result. Figure 2 shows two examples demonstrating the predictive capabilities of our model. We can see that BOP is not only able to distinguish correctly between various bulk magnetic phases of Fe, but it also predicts rather subtle features, such as the structural instability of the NM bcc phase under tetragonal deformation [18]. An extensive lists of validation tests of the potential showing the importance of magnetic effects are given in Ref. [16].

In the following we focus on the properties of dislocations—defects that mediate the plastic deformation at the atomic scale. Studies of dislocations in α -Fe have recently attracted a lot of attention from the materials modeling community, but the influence of magnetic effects on dislocation behavior is still largely unknown. Additionally, it was revealed [23] that the properties of the $1/2\langle 111 \rangle$ screw dislocation, which is known to control the low temperature plastic behavior of all bcc metals, is described poorly by all existing empirical potentials.

We investigated the core structures of both screw and edge dislocations with the $1/2\langle 111 \rangle$ and $\langle 100 \rangle$ Burgers vectors in α -Fe using our magnetic BOP. The resulting structures are shown in Fig. 3 and Ref. [16]. In addition to the core structures our calculations reveal also the changes of local magnetic moments within the cores. For the $1/2\langle 111 \rangle$ screw dislocation these changes are negligible and the core adopts the “nondegenerate” structure, virtually identical to that found in DFT studies [23]. The small variations in magnetic moments of the core atoms are understandable as the main structural changes are in bond angles rather than in bond lengths. In contrast, a

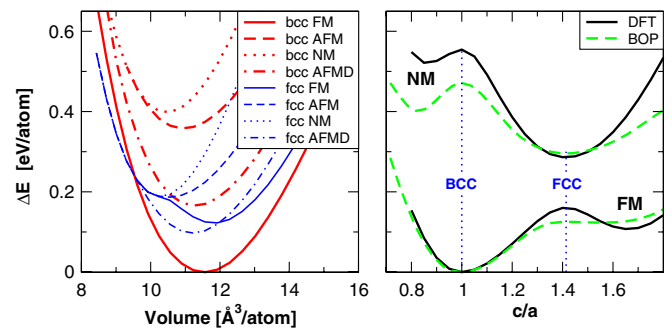


FIG. 2 (color online). Relative stabilities of bcc and fcc Fe bulk phases (left) and the Bain transformation path between the two phases (right) calculated using BOP.

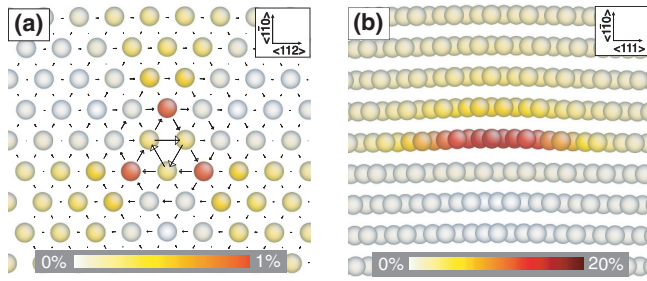


FIG. 3 (color). Core structures of the $1/2[111]$ screw (a) and edge (b) dislocations. The coloring of the atoms shows the relative decrease of atomic magnetic moments from their bulk value.

much larger decrease of the magnetic moments by about 20% of the bulk value is visible in the region of highest compressive stress of the $1/2\langle 111 \rangle$ edge core. Even larger changes occur in the cores of $\langle 100 \rangle$ dislocations [16].

The analysis of the core structures is only the initial step in studies of dislocations. The ultimate goal is to understand their glide behavior under the influence of external stresses. The most interesting is the mobility of the $1/2\langle 111 \rangle$ screw dislocation, whose nonplanar core reacts sensitively to the local stresses and its changes lead to strong variations of the Peierls stress and the operating glide systems, commonly termed as non-Schmid plastic behavior. Recent simulation studies of the $1/2\langle 111 \rangle$ dislocation glide [23,24] were performed mostly with the potential of Ackland and Mendevlev (AM) [2,3] as this has been so far the only empirical potential that yields the nondegenerate core structure. This potential, however, also predicts an occurrence of a metastable dislocation configuration at a halfway position between two minima in the Peierls potential on the $\{110\}$ glide plane and an average dislocation motion on a $\{211\}$ plane even for pure shear stress applied on a $\{110\}$ plane. Both of these predictions disagree with available DFT calculations [23] and experimental observations [25], which identified the screw dislocation to glide at low temperatures exclusively on $\{110\}$ glide planes for arbitrary stress conditions.

We carried out nudged-elastic-band calculations [26] of the energy barrier for the $1/2\langle 111 \rangle$ screw dislocation between its two neighboring equilibrium configurations on the $\{110\}$ plane, which can be considered as an estimate for the Peierls barrier at zero applied stress. A comparison of the results obtained using BOP and the AM potential together with available estimations of the barrier height from DFT calculations and experiments is displayed in Fig. 4. In contrast to the AM potential, BOP yields a barrier with a single maximum located in the halfway position that agrees both qualitatively and quantitatively with available DFT calculations [23] as well as the experimental estimate [25]. The double-hump shape of the energy barrier with a pronounced local minimum in the middle, which corresponds to the metastable dislocation configuration, is a likely unphysical feature originating from deficiencies of the AM potential.

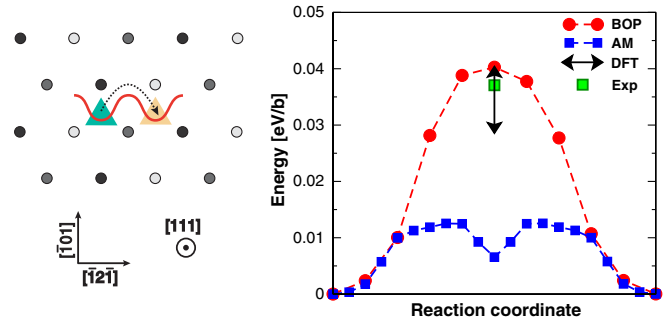


FIG. 4 (color online). An energy barrier associated with the displacement of the $1/2[111]$ screw dislocation by one period along the $[1\bar{2}\bar{1}]$ direction on the $(\bar{1}01)$ plane. A comparison of results computed using BOP, DFT [23], and AM potential with an experimental estimate [25].

On the example of dislocation kinks we demonstrate that BOP is not only robust and reliable but also computationally efficient to carry out large-scale simulations. We note here that calculations of kink energies are a very subtle subject. They require large computational blocks and are prone to be influenced by boundary conditions and elastic effects. This can be demonstrated on the large variation of kink energies obtained with the same interatomic potential [24,27,28]. It should be stressed that the formation energy of a single kink, which is of the order of few tens of eV, need to be obtained as a difference of total energies of large atomic ensembles that typically exceed 10^5 eV. We therefore believe that calculated kink energies should be taken cautiously and considered more for their relative rather than absolute values.

The formation energies of individual single kinks on the $1/2\langle 111 \rangle$ screw dislocation were computed for fully 3D simulation blocks with varying dimensions in directions perpendicular as well as parallel to the dislocation line. Our largest block with a kinked dislocation of a total length of 26 Burgers vectors contained more than 70 000 atoms. The two kinks of a kink pair on the $1/2\langle 111 \rangle$ screw dislocation are not degenerate but have distinct atomic structures. Because of local tensile and compressive regions in the kink center they are sometimes termed as “vacancy” and “interstitial” kinks even though the number of atoms remains constant [24,28]. Our BOP calculations predict the formation energies of the vacancy and interstitial kinks to be 0.62 eV and 0.53 eV, respectively. Even though the results for the largest block sizes seem to be converged with respect to the system size these energies should be taken as upper limits. The lower formation energy of the interstitial kink is related to magnetic effects. According to the BOP results two atoms at the center of this kink flip their magnetic moments to an antiferromagnetic state while in the vacancy kink we observe only marginal changes of the local magnetic moments. Additionally, our simulations show that the kink region is rather compact, which is in contrast to simulations carried out with the

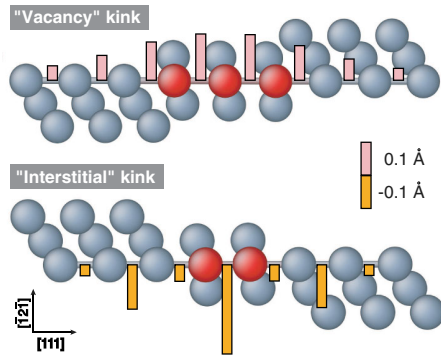


FIG. 5 (color online). Atomic core structures of the two dislocation kinks. The bars correspond to changes of bond lengths of the marked bonds compared to a straight $1/2\langle 111 \rangle$ screw dislocation.

AM potential [28]. This result is again most likely related to the central-force character of the AM potential that favors a conservation of atomic volumes rather than of bond angles. Figure 5 displays the atomic core structures of both kinks computed using BOP. The bars corresponding to the increase (vacancy kink) and decrease (interstitial kink) of the nearest-neighbor bond lengths along the $\langle 111 \rangle$ direction show that the two kinks are distinct. Especially in the interstitial kink, the central bond is reduced due to the magnetic effects by more than 10% while its neighboring bonds have lengths similar to those in the ideal straight dislocation. The prediction of a distinct character of the two kinks is unique to our potential, and the change of the local magnetic state asks for an experimental validation.

In summary, the magnetic bond-order potential for Fe is the first interatomic potential, which is able to describe correctly two crucial ingredients of cohesion and structure in iron—the unsaturated directional covalent bonds and the magnetic interactions. This potential reproduces correctly the relative stability of different magnetic bulk phases as well as the behavior of lattice defects such as dislocations that induce changes in bond lengths, bond angles, and local magnetic moments. At the same time the BOP model remains efficient enough to be applied in atomistic studies of complex defect configurations. Furthermore, its generalization to include additional elements such as carbon or hydrogen is a relatively straightforward task.

This research was supported in part by the DFG Grant No. MR 22/5-1, and by the BMBF Grant No. 03X0511. The work at CCFE is funded by the RCUK Energy Programme, Grant No. EP/I501045, and EURATOM. The authors gratefully acknowledge collaborations and fruitful discussions with D. Pettifor and V. Vitek. We thank M. Reese and B. Meyer for providing us DFT data used for parameterization of the bond integrals and M. Cak for carrying DFT calculations of the Bain transformation.

*matous.mrovec@iwm.fraunhofer.de

- [1] G. Ackland, D. Bacon, A. Calder, and T. Harry, *Philos. Mag. A* **75**, 713 (1997).
- [2] M. Mendeleev, S. Han, D. Srolovitz, G. Ackland, D. Sun, and M. Asta, *Philos. Mag.* **83**, 3977 (2003).
- [3] G. Ackland, M. Mendeleev, D. Srolovitz, S. Han, and A. Barashev, *J. Phys. Condens. Matter* **16**, S2629 (2004).
- [4] S. Dudarev and P. Derlet, *J. Phys. Condens. Matter* **17**, 7097 (2005).
- [5] G. Simonelli, R. Pasianot, and E. Savino, *Phys. Rev. B* **50**, 727 (1994).
- [6] M. Müller, P. Erhart, and K. Albe, *J. Phys. Condens. Matter* **19**, 326220 (2007).
- [7] H. Hasegawa and D. G. Pettifor, *Phys. Rev. Lett.* **50**, 130 (1983).
- [8] A. Bartók, M. Payne, R. Kondor, and G. Csányi, *Phys. Rev. Lett.* **104**, 136403 (2010).
- [9] E. C. Stoner, *Proc. R. Soc. London A* **169**, 339 (1939).
- [10] D. G. Pettifor, *Phys. Rev. Lett.* **63**, 2480 (1989).
- [11] A. P. Horsfield, A. M. Bratkovsky, D. G. Pettifor, and M. Aoki, *Phys. Rev. B* **53**, 1656 (1996).
- [12] *Modelling Electrons and Atoms for Materials Science, Prog. Mater. Sci.*, edited by R. Drautz and M. Finnis (Elsevier, Oxford, 2007), Vol. 52(2–3).
- [13] M. Mrovec, D. Nguyen-Manh, D. G. Pettifor, and V. Vitek, *Phys. Rev. B* **69**, 094115 (2004).
- [14] M. Mrovec, R. Gröger, A. Bailey, D. Nguyen-Manh, C. Elsässer, and V. Vitek, *Phys. Rev. B* **75**, 104119 (2007).
- [15] M. J. Cawkwell, D. Nguyen-Manh, C. Woodward, D. G. Pettifor, and V. Vitek, *Science* **309**, 1059 (2005).
- [16] See supplemental material at <http://link.aps.org/supplemental/10.1103/PhysRevLett.106.246402> for details of the BOP model.
- [17] W. Zhong, G. Overney, and D. Tomanek, *Phys. Rev. B* **47**, 95 (1993).
- [18] G. Liu, D. Nguyen-Manh, B.-G. Liu, and D. Pettifor, *Phys. Rev. B* **71**, 174115 (2005).
- [19] A. T. Paxton and M. W. Finnis, *Phys. Rev. B* **77**, 024428 (2008).
- [20] A. T. Paxton and C. Elsässer, *Phys. Rev. B* **82**, 235125 (2010).
- [21] G. Madsen, E. McEniry, and R. Drautz, *Phys. Rev. B* **83**, 184119 (2011).
- [22] D. Nguyen-Manh and S. L. Dudarev, *Phys. Rev. B* **80**, 104440 (2009).
- [23] L. Ventelon and F. Willaime, *J. Comput.-Aided Mater. Des.* **14**, 85 (2007).
- [24] J. Chaussidon, M. Fivel, and D. Rodney, *Acta Mater.* **54**, 3407 (2006).
- [25] D. Caillard, *Acta Mater.* **58**, 3493 (2010).
- [26] G. Henkelman and H. Jónsson, *J. Chem. Phys.* **113**, 9978 (2000).
- [27] D. Terentyev and L. Malerba, *Comput. Mater. Sci.* **43**, 855 (2008).
- [28] L. Ventelon, F. Willaime, and P. Leyronnas, *J. Nucl. Mater.* **386**, 26 (2009).